Spectral Characteristics and Colloidal Properties of Chlorophyll *a*′ in Aqueous Methanol

Toru Oba

Department of Bioscience and Biotechnology, Faculty of Science and Engineering, Ritsumeikan University, Kusatsu, Shiga 525-77, Japan

Mamoru Mimuro[†]

National Institute for Basic Biology, Okazaki, Aichi 444, Japan

Zheng-Yu Wang and Tsunenori Nozawa

Department of Biochemistry and Engineering, Faculty of Engineering, Tohoku University, Sendai 980-77, Japan

Shoichiro Yoshida and Tadashi Watanabe*

Institute of Industrial Science, University of Tokyo, Tokyo 106, Japan

Received: October 18, 1996; In Final Form: February 11, 1997[⊗]

The "phase behavior" of chlorophyll *a*′ (Chl *a*′, C13[2]-epimer of Chl *a*) dissolved in aqueous methanol was examined in terms of the composition of the solvent. This study aimed at elucidating the property of Chl *a*′, the exotic pigment found in a photosynthetic reaction center complex, as well as at clarifying the nature of the Chl aggregation in aqueous media. Visible absorption, circular dichroism (CD), fluorescence and resonance Raman spectroscopies, dynamic light-scattering measurements, and electron microscopy were utilized. Chl *a*′ formed either of two types of colloids depending on the solvent composition. The one formed over a wide methanol volume percentage (ca. 73−30%) commonly possessed a single microscopic structural unit that yielded the double-peaked absorption (ca. 690 and 715 nm) accompanied by a symmetric dispersed-type CD spectrum. Increasing methanol concentration within this solvent composition range enhanced the size of the colloid and finally caused critical opalescence, which was reminiscent of the critical behavior of the aqueous solution of nonionic surfactants. These findings indicate that the microscopic structure of the Chl *a*′ aggregate was independent of the size and shape of the colloid. This is in sharp contrast to the solvent composition dependence of the Chl *a* aggregation in the same medium: an increase in methanol concentration in going from 40% to 70% (vol/vol) shifted a broad red-most absorption band from ca. 700 to 750 nm, which was correlated to the enhancement of the aggregation number and the colloidal size. The difference between the aggregation behaviors of Chl *a* and *a*′ suggests a narrower choice of possible molecular arrangements in the Chl *a*′ aggregate as an inherent property of the pigment. The nature of the Chl aggregation in aqueous media is discussed in relation to the micellization of nonionic surfactant.

Introduction

The primary process of photosynthesis is a light-induced redox reaction driven by chlorophylls (Chls) or bacteriochlorophylls (BChls). These pigments absorb sunlight in light-harvesting (or antenna) pigment−protein complexes and transfer the energy to reaction center (RC) complexes where Chls (BChls) initiate electron transfer. As demonstrated by recent crystallography, the primary donor is composed of two BChl (Chl) molecules,[1−3] and the antenna comprises a larger number of the pigments.[4−6] Chl (BChl) molecules constituting the primary donors or antennas clearly cooperate with each other. These can be regarded as supramolecules, as judged from the red-shifted absorption, and be approximated as aggregates.

The aggregation of Chls in aqueous organic solvents has primarily been studied to mimic the red-shifted absorption spectra in vivo and later to clarify the function of the primary donor and the antenna complex.[7−21] The Chl aggregation in aqueous media still remains ambiguous in contrast to those formed in nonpolar solvents[22,23] or in surfactant micelles.[24] The ambiguity may come from the following three points: (1) Chls generally form colloids at micromolar concentrations in aqueous media;[8−13] (2) substantial information of the colloid was hardly regarded, while visible absorption spectrum was valued to make a comparison between the results obtained in vitro and in vivo; (3) the aggregation (colloid formation) strongly depends on the condition, e.g., the composition of the solvent, and the process is sometimes irreversible, less reproducible, and not simple. The properties of Chl on the aggregation, together with closely correlated issues of the structure of the aggregate, the mechanism of the aggregation, and the properties of the solvent, can be clarified through the examination for not only the spectral characteristics but also the phase behavior of the system. Here, various spectroscopies probing into the microscopic molecular arrangement of the aggregate must be combined with techniques to clarify the colloidal (macroscopic) structure. Such a comprehensive study has not been reported to date.

We studied the aggregation of Chl *a*′ (C13[2] epimer of Chl *a*, Figure 1) in aqueous methanol[20,21] to elucidate the in vivo

* To whom correspondence should be addressed: Institute of Industrial Science, University of Tokyo, Roppongi, Minato-ku, Tokyo 106, Japan; phone and fax: +81-3-3401-5975; e-mail: watanabe@cc.iis.u-tokyo.ac.jp.

† Present address: Department of Physics, Biology and Informatics, Faculty of Science, Yamaguchi University, Yoshida, Yamaguchi 753, Japan.

⊗ Abstract published in *Advance ACS Abstracts,* March 15, 1997.

S1089-5647(96)03227-0 CCC: $14.00

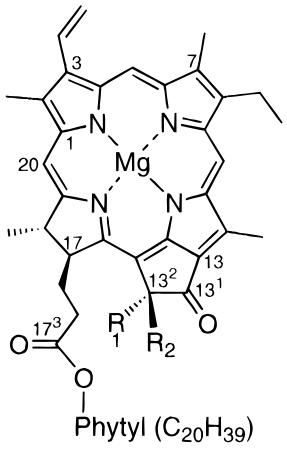

	Chl *a*′	Chl *a*
R_1	H	COOMe
R_2	COOMe	H

Figure 1. Molecular structure of Chl *a* (R^1 = $COOCH_3$, R^2 = H) and Chl *a*′ (R^1 = H, R^2 = $COOCH_3$) with partial carbon numbering according to the IUPAC system.

function of the two Chl *a*′ molecules found in the core part of the RC of photosystem (PS) I.[25] A unique aggregate of Chl *a*′ formed through simple transformation from one species to another in a particular mixed solvent of methanol/water (40/60, vol/vol),[20] in marked contrast to the heterogeneous aggregation behavior of Chl *a* in a common medium.[14−16] It was not necessarily clear that the difference arose from the unique property of Chl *a*′; under other conditions, Chl *a*′ might show a heterogeneous aggregation behavior including the formation of higher aggregates that could be related to a broad absorption accompanied with an absorbance tailing given by the Chl *a*′ aggregate formed in a methanol/water (60/40, vol/vol) medium.[21]

In this work, we examined the aggregation behavior of Chl *a*′ in detail in terms of the effect of the solvent (aqueous methanol) at a fixed temperature of 25 °C. The primary incentive was to clarify the property of Chl *a*′. Another was to give a basis for the consideration of the nature of the Chl aggregation in aqueous media. The microscopic and macroscopic structures of the Chl *a*′ aggregate colloids in aqueous methanol were studied by visible absorption, circular dichroism (CD), fluorescence and resonance Raman spectroscopies, dynamic light-scattering (DLS) measurements, and transmission electron microscopy (TEM). The results were put together to yield a "phase diagram" in terms of a "unit structure" of the aggregate colloid.

Materials and Methods

Materials. The preparation of Chl *a*′ was described elsewhere.[20,26] Briefly, Chl *a*′ was obtained by partial epimerization of Chl *a* extracted from lyophilized spinach leaf tissues. Pigments were isolated by a preparative normal-phase HPLC (column consisting of Senshupak silica-5251N, 20 mm in diameter × 250 mm at 4 °C; eluent consisting of hexane/2-propanol/methanol = 100/0.8/0.4). A prescribed amount of Chl *a*′ (about 25 nmol pigment, purity >99%) was stored in 5 mL glass vials in solid form at −30 °C until use. The integrity of the pigment was ensured by analytical silica HPLC (column consisting of Senshupak silica-1251N, 4.6 mm in diamter × 250 mm at 4 °C; eluent consisting of hexane/2-propanol/methanol = 100/0.8/0.4), visible absorption, CD, elemental analysis, ^{1}H NMR, and FAB-MS.[26,27]

HPLC-grade hexane, methanol, and 2-propanol and reagent-grade chloroform were from Wako Pure Chemicals, Ltd. and used without further purification. Water purified with a Milli-Q system (Millipore Ltd.) was used throughout.

Preparation and Spectroscopy of Chl *a*′ Aggregate. In what follows, the solvent composition is denoted by the methanol (M) volume percentage as, for example, M 40%. A prescribed amount of methanol was put into a vial to dissolve the pigment, and the solution was diluted quickly with water followed by stirring for 3 min (1 min for relatively unstable solutions formed in M 73−60%). Several milliliters of the solution (nearly 5 μM on the monomer basis) was taken into a cuvette, and the absorption spectral transformation was monitored at appropriate time intervals. The cuvette was thermostated at 25 °C, and all the operations were done under dim green light.

A JASCO spectrophotometer Model UVIDEC-660 and a Hitachi spectrophotometer Model 330 were employed to record the absorption spectra. Circular dichroism (CD) and fluorescence measurements were performed on a JASCO spectropolarimeter Model J-200B and a Hitachi fluorescence spectrophotometer Model 850, respectively. The fluorescence quantum yield of Chl in an M 80% medium was estimated based on the literature value of 0.23 in neat methanol.[28] Resonance Raman spectra were measured with 5 cm^{-1} resolution by use of a 457.9 nm line of an Ar^+ laser (NEC GLG-3460, <10 mW) and a JASCO Raman spectrometer R-800. The concentration of the sample solution was 50 or 100 μM, prepared by the same way as described above.

A light-scattering spectrometer DLS-600 (Otsuka Electronics) was employed to obtain distributions of hydrodynamic diameters of the aggregate colloids at 25 °C. The sample with a concentration of 10 μM was irradiated by a 5 mW He−Ne laser, and a photomultiplier was set at a scattering angle of 90°. The data obtained were analyzed by the histogram method on an NEC PC-9801 DA. Transmission electron microscopy (TEM) was performed on a Hitachi electron microscope Model H-800 operated at 150 kV. Precipitates of the aggregate formed in M 40% were collected by centrifugation (30 000−40 000 rpm, 30 min, 25 °C) of a relatively concentrated solution (20 μM on the monomer basis, 25 °C). The film of the M 60% aggregate was formed on the solution surface by vibration. The samples were placed on a collodion-coated 400-mesh copper grid.

After spectroscopic measurements, the pigment was extracted with chloroform to examine the molecular integrity by the analytical HPLC mentioned above.

Results

Visible Absorption Spectrum of Chl *a*′ in Aqueous Methanol. Figure 2a depicts visible absorption spectra of Chl *a*′ recorded at stationary state for various solvent compositions (25 °C and 6 μM). Absorption maxima and ratio of absorbances (*A*) at 800 and 716 nm are plotted in Figure 2b as a function of the solvent composition. Above M 73%, Chl *a*′ is dispersed as monomer. At M 80%, for instance, the Q_y band peaks at 666.4 nm with a bandwidth (full width at half-maximum, fwhm) of ca. 520−525 cm^{-1} and a molar extinction coefficient of (7.1−7.5) × 10^4 M^{-1} cm^{-1}. The Q_y maximum is ca. 0.6 nm red-shifted compared with that of Chl *a*, probably arising from minor strain in the molecular structure. These characteristics are almost identical with those of monomeric Chl *a*′ in neat methanol.

A characteristic is a double-peaked absorption spectrum developing over the solvent composition range of ca. M 70% to M 40%. The location of the doublet is almost independent

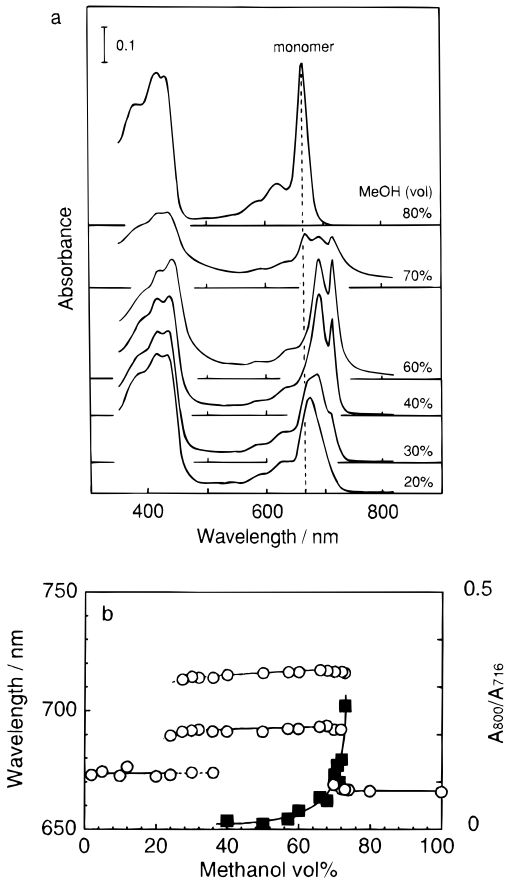

Figure 2. (a) Solvent composition dependence of the stationary visible absorption spectrum of the Chl *a*′ aggregate in aqueous methanol (6 μM on the monomer basis, 25 °C). (b) Plots of absorption maxima and absorbance ratio against solvent composition (4−6 μM on the monomer basis, 25 °C): (○) absorption maxima in the red region; (■) ratio of absorbance at 800 and 716 nm.

of the solvent composition (690−693 and 714−717 nm; see Figure 2b), though it could depend on an increase in dielectric constant of the solvent (50 at M 70% to 68 at M 40%). The doublet grows at the expense of the monomeric Q_y band (666 nm) in going from M 73% to ca. M 60%. A decrease in M% from M 60% to M 40% reduces the intensity of the lower energy band of the doublet relative to the higher energy one. Concomitantly, the spectral shape becomes sharper (440 and 260 cm^{-1} in fwhm for the doublet at M 40%), and the absorbance tailing extending beyond 800 nm becomes less intense as demonstrated by a decrease in A_{800}/A_{716} (Figure 2b). The tailing developed in pace with the evolution of the doublet, and the ratio of A_{800}/A_{716} remained constant over a concentration range of 0.25−20 μM at M 60% (data not shown). The Chl *a* aggregation also exhibited a large red-shift in the same solvent composition region (see Figure 9 and refs 14−16).

The double-peaked component diminishes as the methanol concentration decreased from M 40% to M 20% and is no longer observed in the range below ca. M 20%. A spectral component dominating instead is a broad "triangular" absorption, tailing toward the longer wavelength region. The absorption maximum is at around 672 nm, and the bandwidth (fwhm) is ca. 800 cm^{-1}. Such a feature was commonly observed even at M 10%, M 5%, and M 2% (data not shown). Note that the spectral transformation in going from M 20% to M 30% and to M 40% is quite similar to the temporal evolution of the absorption spectrum of the M 40% aggregate.[20]

As clearly shown in Figure 2b, Chl *a*′ seems to take one of three forms depending on the solvent composition. In what follows, we analyze the species at the representative solvent compositions of M 20%, M 40% (almost no absorbance tailing), M 60% (clear absorbance tailing), and M 80%.

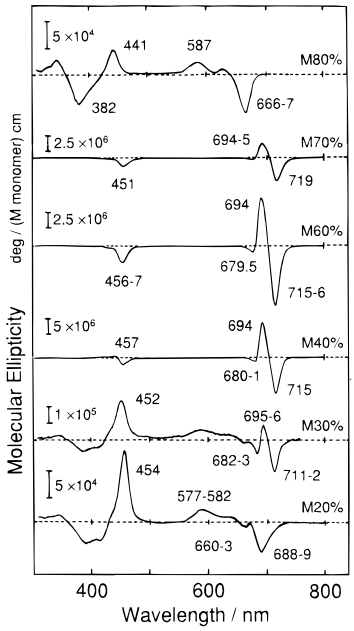

Figure 3. Solvent composition dependence of the stationary CD spectrum of the Chl *a*′ aggregate in aqueous methanol (4.9 μM on the monomer basis for M 70−30%, 19 μM for M 80%, and M 20%; 25 °C).

CD Spectra. Figure 3 shows CD spectra of the Chl *a*′ species at the representative solvent compositions (4.9 μM on the monomer basis). Chl *a*′ in the M 80% medium gives a CD spectrum identical with the monomeric one in neat methanol; the Q_y trough is at 666−667 nm (molecular ellipticity, -7.0×10^4 deg M^{-1} cm^{-1}) and the Soret peak at 441 nm ($+4.6 \times 10^4$ deg M^{-1} cm^{-1}). The Q_y bandwidth was 650 cm^{-1} (fwhm).

A dispersed-type component (CD couplet) was commonly observed in the red region over a wide solvent composition range of M 70% to 30%. The peak positions of the CD couplet remains nearly constant at 694−695 and 715−716 nm, roughly coinciding with those of the doublet in the absorption spectra (Figure 2a). The polarity of the couplet is also independent of the solvent composition (positive for the higher energy component). Decreasing M% from M 70% to M 40% intensifies and sharpens the spectrum, as in the absorption spectrum. As typical examples, the amplitudes (calculated on the basis of monomer concentration) and the bandwidths (fwhm, in parentheses) were $+7.6 \times 10^6$ deg M^{-1} cm^{-1} (440 cm^{-1}) and -9.7×10^6 deg M^{-1} cm^{-1} (300 cm^{-1}) for the M 60% aggregate and $+1.1 \times 10^7$ deg M^{-1} cm^{-1} (310 cm^{-1}) and -1.1×10^7 deg M^{-1} cm^{-1} (270 cm^{-1}) for the M 40% aggregate.

The aggregate species formed in M 20% gives a CD spectrum that is similar to the spectrum of the monomer except for a few differences. The Q_y absorption gives rise to a broad "triangular" trough at 688−689 nm (510 cm^{-1} in fwhm), 12 nm red-shifted from the monomeric Q_y band observed at M 80%. The positive component in the Soret region (454 nm) is 13 nm red-shifted and 2.8-fold intensified compared with the monomer's. It is supposed that a combination of the M 20%-type and the M 40%-type spectra yields an intermediate spectral pattern of the M 30% aggregate, though the double-peaked component was barely detectable in the absorption spectrum of this particular M 30% sample.

Fluorescence Spectra. Figure 4 exhibits the solvent composition dependence of the fluorescence spectrum of Chl *a*′ (0.02

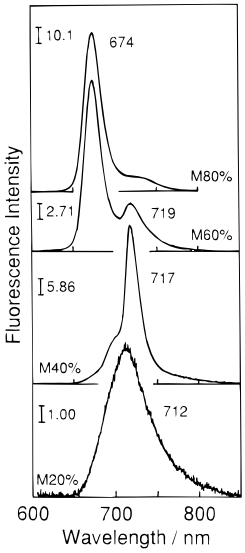

Figure 4. Solvent composition dependence of fluorescence emission spectrum of the Chl *a*′ aggregate in aqueous methanol at 25 °C: (M 80%) 0.02 μM, λ_{ex} = 432 nm; (M 60%) 4.9 μM, λ_{ex} = 442 nm; (M 40%) 4.9 μM, λ_{ex} = 440 nm; (M 20%) 4.9 μM, λ_{ex} = 432 nm.

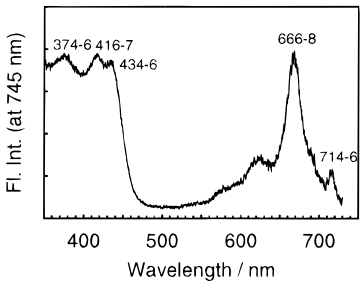

Figure 5. Fluorescence excitation spectrum of the Chl *a*′ aggregate formed at M 60% (4.9 μM on the monomer basis, 25 °C, λ_{ex} = 745 nm).

μM for the M 80% sample and 4.9 μM for the others). The spectrum obtained at M 80% is again nearly identical with that at M 100% (neat methanol). The Q_y (0−0) band is located at 674 nm with a bandwidth (fwhm) of ca. 540 cm^{-1} (the Stokes shift, 165 cm^{-1}). The quantum yield was 0.25.[28] The position of the fluorescence maximum is 0.6 nm red-shifted from that of Chl *a*, consistent with the absorption spectrum. A minor band arising from the Q_y (0−1) transition is also observed. The fluorescence excitation measurement, detected at 740 nm, gave a sharp band peaking at 667−668 nm (data not shown).

The Chl *a*′ aggregate formed at M 60% exhibits a 674 nm fluorescence band with a minor peak at 719 nm. A trace amount of monomer that escaped the aggregation gave the former band as judged from the fluorescence excitation spectrum (data not shown). Excitation at wavelengths longer than the Soret absorption maximum (450−465 nm) enhanced the other spectral component at 719 nm (see Figure 10a), and so did excitation at 692 nm where the higher energy band of the doublet peaks at. On the other hand, excitation at 668 nm (at around the monomeric Q_y maximum) resulted in a decrease in the intensity of the 719 nm fluorescence. Even the 465 nm excitation did not give rise to any new emission band in the wavelength region above 719 nm. The fluorescence excitation spectrum of the M 60% aggregate (Figure 5, detected at 745 nm) reveals a small absorption at 714−716 nm as well as a slight shoulder component on the blue side of the monomeric Q_y band (at 690−700 nm).

The M 40% aggregate yields fluorescence at 717−718 nm with a bandwidth (fwhm) of 420 cm^{-1}. A minor emission band exists at 690−700 nm, while the monomer's fluorescence is significantly diminished. The dominant 718 nm band was attributed to a transition from the lower energy part of the exciton-split S1 states of the aggregate, and the small shoulder component (690−700 nm), to that from the higher energy one.[20]

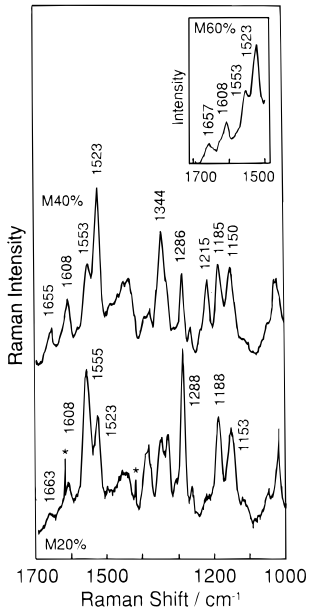

Figure 6. Solvent composition dependence of resonance Raman spectrum of the Chl *a*′ aggregate in aqueous methanol (100 μM for M 20% and 40% and 50 μM for M 60% on the monomer basis; room temperature).

The fluorescence spectrum of the M 20% aggregate is less intense and broader than others. The fluorescence maximum was at around 712 nm, and the bandwidth (fwhm) was 1450 cm^{-1}. The shape and the amplitude of the spectrum resemble those of the precursor of the doublet-giving aggregate formed at M 40%.[20] Similarity was also noted in the fluorescence excitation spectra; both aggregates revealed "triangular" spectra that peaked at around 670 nm and tailed off into the 720 nm region as in the absorption spectra (data not shown).

Resonance Raman Spectra. Figure 6 depicts the resonance Raman spectra of the Chl *a*′ aggregates. The sample concentrations were 100 μM for the M40% and the M 20% aggregates and 50 μM for the labile M 60% aggregate. There was little difference in peak positions and spectral features except for a slight broadening when the absorption spectra of these concentrated solutions were compared with those obtained at 5 μM (Figure 2a). Therefore, it is suggested that the Raman spectra obtained at such high concentrations reflect the microscopic structure of the aggregates present at lower concentrations around 5 μM.

Both of the Chl *a*′ aggregates formed at M 60% and M 40% show essentially identical Raman spectra. The location of three bands at 1523, 1553, and 1608 cm^{-1}, originating from the C=C stretching mode of the chlorin macrocycle, indicates the five-coordinated state of the central Mg atom.[29] The carbonyl stretching vibration of the C13^1-keto moiety gives rise to the scattering band at around 1655 cm^{-1}, downshifted from that of the coordination-free keto group or even the hydrogen-bonded one.[30] The constituent Chl *a*′ molecules of the M 60% aggregate probably associate as those of the M 40% aggregate do.[20]

Even for the M 20% aggregate, the wavenumber positions of the coordination-sensitive bands (1523, 1555, and 1608 cm^{-1}) and the C13^1-keto carbonyl band (1665 cm^{-1}) are nearly equal to those of the M 60% and the M 40% aggregates, indicating the common molecular linkage. Note that the scattering

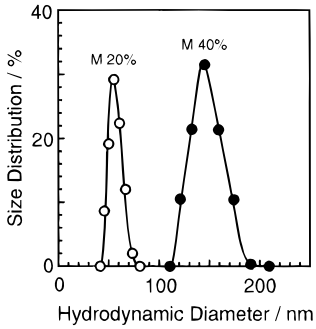

Figure 7. Distribution of hydrodynamic diameter of the Chl *a*′ aggregate formed at M 20% and M 40%.

intensity pattern of the spectrum is different between the M 20% and the M 40% aggregates; one can find a change in the relative amplitudes of the 1553 and the 1523 cm^{-1} bands, the presence or absence of the 1215 cm^{-1} band, an increase or a decrease in the intensity of the 1288 cm^{-1} band, and additional differences in the range 1300−1400 cm^{-1}. The M 20%-type feature had also been observed for Chl *a* monomer, for the Chl *a* aggregates formed in dry nonpolar solvents, and for the precursor colloid of the M 40% Chl *a*′ aggregate.[20,29,30]

Colloidal Properties of the Chl a′ Aggregates. The size of the aggregate colloid enhanced with increasing M% as demonstrated by the dynamic light scattering (DLS) measurements. Figure 7 illustrates the size distribution histograms of the Chl *a*′ aggregates formed at M 20% and M 40%. The M 20% aggregate revealed a narrow distribution peaked at around 50 nm (mean diffusion coefficient of 6×10^{-8} cm^2 s^{-1}). Similar results were obtained for the M 10% aggregate colloid and the species formed at the initial stage of the M 40% aggregation, both of which gave the "triangular" absorption. The average hydrodynamic diameter of the doublet-giving M 40% aggregate was ca. 130 nm, independent of the concentration over the range 5−100 μM. The mean diffusion coefficient was 2×10^{-8} cm^2 s^{-1}. This mature 130 nm colloid developed at the expense of the precursor 50 nm colloid. The size of the aggregate formed at M 50%, 60%, and 70% may not be smaller than the wavelength of the incident light (632.8 nm). The last two solutions especially showed anomalous fluctuation of scattering light, which hampered accurate particle size determination.

The macroscopic feature of the Chl *a*′ aggregate colloids was observed by transmission electron microscopy (TEM). The electron micrograph of the M 40% aggregate showed spherical or ellipsoidal particles of 100−200 nm in diameter. There also existed some larger particles whose shape was like a string of beads possibly formed by coalescence of the smaller particles during the centrifugation. Figure 8 exhibits the electron micrograph of the aggregate film formed on the surface of the M 60% solution. A random network structure characteristic of a gel was unambiguously noted. The thickness of the thread of the network seems to be 100−300 nm.

The M 40% aggregate can be transformed into monomer by increasing M% to 80%. However, it was impossible to convert the absorption spectrum of the M 40% aggregate into that of the M 60% by addition of methanol. Also, the absorption spectral shape hardly transformed by dilution of the M 40% solution with water. Addition of methanol or water to the M 60% solution resulted only in the formation of films or precipitation. Similar behavior was reported previously.[14,15,18]

Both the growth speed and the stability of the colloid depended on the solvent composition. The aggregation was facilitated under a more hydrophobic condition within the range M 70%−30%, though the resulting solution was less stable.

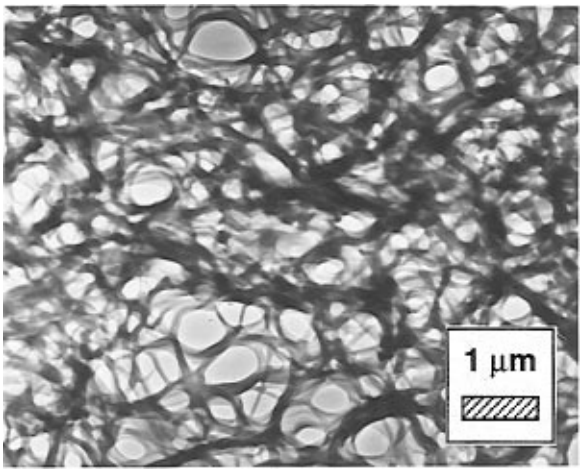

Figure 8. Electron micrograph of a film of the M 60% aggregate formed on the solution surface (×10 000).

The double-peaked spectrum at M 70% grew very rapidly (within 30 min from admixing of water) but easily faded because of precipitation or film formation. The M 60% aggregation completed within 60 min, and the formed colloid did not precipitate until stirring or vibration was given to the solution. These aggregate solutions were turbid in contrast to those at M 40% and 30%. Much longer time (15−20 h) was required for the M 40% aggregation. The M 40% aggregate stayed static even when the mechanical energy was given to the solution. The spectral transformation was very slow and less reproducible at around M 30%.

Pigment Integrity of the Chl *a*′ Aggregates. Little degradation occurred during the experiments over the solvent composition region from M 70% to 40% where the double-peaked absorption was clearly noted. The 2 h experiment for the M 60% and the M 57.1% aggregations resulted in only slight decreases in the purity from 99.8% to 99.4% and to 98.5%, respectively. The M 40% aggregation also kept the pigment integrity even during the 20 h aggregation (final purity of 97.9%).[20] On the other hand, monomeric Chl *a* and *a*′ (above ca. M 70%) and the Chl *a*′ aggregate formed in the solvent composition range below ca. M 30% hardly held the initial purity for 2−3 h.[31]

Chl *a* Aggregation in Aqueous Methanol. Chl *a* showed a heterogeneous aggregation behavior in aqueous methanol (Figure 9). Chl *a* forms aggregates below M 74%. The aggregates gave the red-most absorption at around 700 or 750 nm in the solvent composition range from ca. M 70% to 40%, and below M 40% the "triangular" spectral component (peaking at ca. 670 nm) becomes dominant with a small band at around 700 nm. This behavior was in line with those reported previously,[14−16] though these were not necessarily coincident with each other at a common solvent composition because of poor reproducibility and a difference in incubation time. Prolonged monitoring (several hours to a few days) revealed to us that the Chl *a* aggregate systematically diminishes the bathochromic shift of the red-most band with decreasing M%: 760−770 nm at M 70% to around 700 nm at M 40%. Jacobs et al. studied the aggregation of ethyl chlorophyllide *a* in aqueous acetone by visible absorption spectroscopy and electron microscopy and showed that the bathochromic shift of the Q_y band decreased logarithmically with decreasing crystal size.[11] The simulations demonstrated that the bathochromic shift of several Chl aggregates changes with the aggregation number for a given pigment array.[32,33] These strongly suggest that increasing M% enhanced the Chl *a* aggregate colloid.

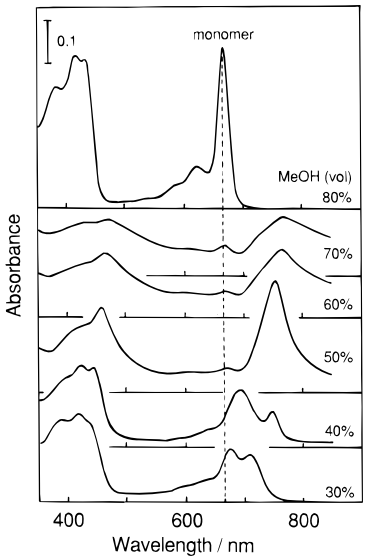

Figure 9. Solvent composition dependence of the stationary visible absorption spectrum of the Chl *a* aggregate in aqueous methanol (5 μM on the monomer basis, 25 °C).

Such a changeableness of the Chl *a* aggregates is responsible for poor reproducibility, and the coexistence of several aggregate forms even under a fixed condition. The appearance of the 750 nm absorbing species in M 40% depended quite delicately on the details of experimental conditions, whereas the M 50% solution exhibits a complex CD spectrum composed of several positive and negative components in the wavelength range of the intense 750 nm absorption band (data not shown).

Discussion

Nature of the Doublet-Giving Species. As clearly shown in the above section, Chl *a*′ is dissolved as monomer in the relatively hydrophobic solvent composition region, whereas the pigment forms the 50 nm colloid particle that gives the "triangular" absorption under very hydrophilic conditions. The question that requires discussion is the aggregation behavior in the solvent composition region where the doublet was noted. Figure 10a illustrates a deconvolution pattern of the fluorescence emission spectrum of the M 60% aggregate. The measured spectrum A, obtained by the 465 nm excitation, is well interpreted as a combination of the monomeric contribution (component B, obtained at M 80%) and component C arising from the aggregate. Component C is quite similar to the emission spectrum of the M 40% aggregate, which showed a sharp band peaking at 717−718 nm accompanied by a slight shoulder component at 690−700 nm (Figure 4). Figure 10b is a fraction of the fluorescence excitation spectrum originating from the M 60% aggregate as estimated by subtraction of the monomer's contribution (ca. 0.3% of the initial concentration using the spectrum obtained at M 80%) from the observed spectrum (Figure 5). Extracted is a double-peaked component peaking at around 690 and 715 nm, which is reminiscent of the absorption and the fluorescence excitation spectra of the Chl *a*′ aggregate formed in the M 40% medium.[20] The present analyses indicate that the double-peaked absorption observed in the system arises basically from the common origin.

There is no evidence for a higher aggregate (or a microscopic structure where Chl molecules are coupled more strongly than in the doublet-yielding species) that could be responsible for the absorbance tailing. The higher aggregate, if any, could give rise to a fluorescence band beyond 720 nm with excitation at a wavelength longer than the Soret absorption maxima because

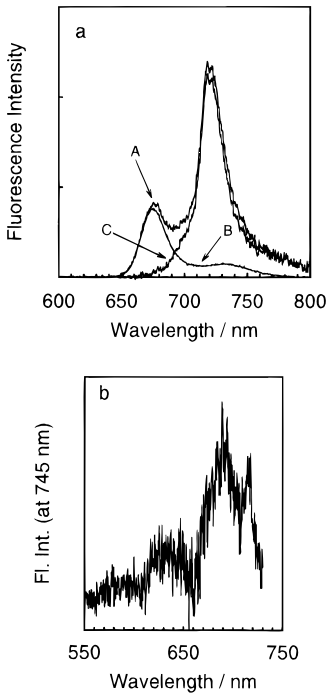

Figure 10. (a) Deconvolution of fluorescence spectrum of Chl *a*′ at M 60%: (A) observed spectrum excited at 465 nm; (B) contribution from monomer; (C) contribution from the aggregate. (b) Contribution of the Chl *a*′ M 60% aggregate to the fluorescence excitation spectrum (extracted by subtraction of monomer's spectrum obtained at M 80% from Figure 5).

several aggregate forms including the 750 nm absorbing polymer fluoresce (ref 34 and Oba et al.'s unpublished results). The absence of the far-red absorbing species was also demonstrated by the second and fourth derivative of the absorption spectrum (data not shown). The finding that the proportion of the absorbance tailing to the doublet was unchanged with concentration conflicts with a possible process that the doublet-giving species further associates to form the higher aggregates.

The DLS and TEM measurements for the Chl *a*′ aggregates revealed the increase in the colloidal size in going from M 20% to 60% and the anomaly of scattered light intensity at M 60% and M 70% where the gelation readily occurred. This trend is similar to the critical behavior of the aqueous solution of nonionic surfactants.[35] As the hydration of the nonionic surfactant molecule becomes harder, e.g., by the increase of temperature, the micelles coalesce to form larger aggregates, resulting in a phase separation into a swollen surfactant phase and a water phase dissolving a small amount of monomeric surfactant.[36] Anomalous fluctuation of scattering light called critical opalescence is a common observation near the phase transition point. In view of the weakening of the hydrogen bonding, an increase in M% corresponds to a rise of temperature. Thus, the heavy absorbance tailing in question is rationalized as light reflection by the large colloidal particles, which can be regarded as phase separation.[11] This is consistent with the finding that the absorbance ratio A_{800}/A_{716} increased with the colloidal size (Figure 2b). The broader spectrum in M 60% may reflect a swollen gel structure in which the molecular motion is suppressed to a lesser extent than in the relatively packed structure of the M 40% aggregate.

Phase Diagram in View of the Unit Structure of the Aggregate Colloid. The above consideration clearly shows that the microscopic structure of the Chl *a*′ aggregate yielding the double-peaked absorption is independent of the size and shape of the colloid. This is in sharp contrast to the Chl *a* aggregation

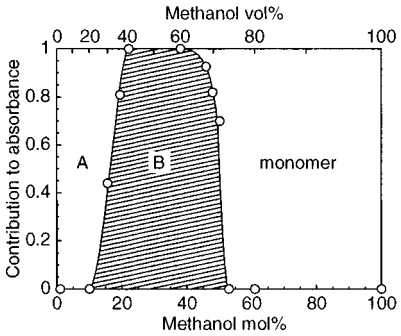

Figure 11. Diagrammatic representation of the solvent composition dependence on the Chl *a*′ aggregation in aqueous methanol based on the data in Figure 2 (ca. 5 μM, 25 °C). The contribution from structure B was normalized at M 60% and M 40% where almost no residual monomer (or structure A) was detected. The monomer's contribution at around M 70% was estimated by fitting of the Q_y band, and the remaining part was attributed to structure B. Another boundary (ca. M 30%) was placed based on the time course of the M 40% aggregate spectra that were deconvoluted with the M 20%- and the M 40%-type spectra, both normalized at the respective absorption maximum in the red region (see ref 20). Note that area A should not include M 0% because Chl is not dissolved in pure water.

in aqueous media. The unique feature of the Chl *a*′ aggregation could be related to a "unit structure" of the colloid defined as the minimal molecular array that gives the spectroscopic properties. The size of the unit structure is regarded as an area where electrons can delocalize. It is assumed that such units coalesce at random to form the colloid or the macroscopic structure. As shown in the previous report, the broad "triangular" spectrum and the double-peaked absorption observed in the M 40% aggregation were well approximated to arise from the respective single aggregate species. We tentatively supposed the precursor to be T-shaped oligomers whose component molecules are loosely coupled with each other and the product to be an anhydrous aggregate composed of stacked macrocycles.[20] Now we find that these, corresponding to the unit structures, are crucial for the Chl *a*′ aggregation not only under a fixed condition of M 40%. We call the structure of the components of the T-shaped oligimers structure A and call the structure of the stacked macrocycles structure B in what follows.

Thus, Chl *a*′ in aqueous methanol is regarded as existing in the form of structure A, structure B, or a monomer depending on the solvent composition, in the first approximation. The results are represented in Figure 11, showing a sort of phase diagram in terms of the contribution of each structure to the overall absorbance. The contribution from structure B was normalized at M 60% and M 40% where almost no residual monomer or structure A is detected.[20] Structure A is formed not only in area A in Figure 11 but in the water-rich side of area B as the precursor of structure B. Structure A may be a universal form of Chls in hydrophilic media. Very similar spectral components are observed also for the Chl *a* aggregation in aqueous alcohol,[14−16] aqueous dioxane,[9] and aqueous dimethyl sulfoxide.[18]

Conclusion

The heterogeneity in the Chl *a* aggregation probably arises from the property of the pigment that allows a wide variety of unit structures on the aggregation. The ternary molecular linkage characteristic of ethyl chlorophyllide *a* dihydrate crystal allows a three-dimensional extension.[37] In contrast, the homogeneity in the Chl *a*′ aggregation may suggest that the possible structure of the aggregate is significantly restricted as an inherent property of Chl *a*′. The size of unit structure B is not clear at this experimental stage. One possibility is a dimer,[20] which may be suggestive of the yet unknown function of the in vivo Chl *a*′.

Not only the Chl *a*′ aggregation presented above but the Chl *a* aggregations in aqueous methanol (Figure 9) and in aqueous dimethyl sulfoxide[18] seem to present a similar "phase diagram" composed of three areas. They commonly showed the monomer's area, an area corresponding to area *A*, and one where a pronounced red-shifted absorption was noted (corresponding to area B), except for differences in the formed far-red absorbing species and in the boundary solvent compositions. Thus, the effect of the solvent on the Chl aggregation and, hence, the mechanism of the Chl aggregation may be common in every aqueous media. The Chl aggregation in aqueous organic solvents is similar to a phase separation (a micellization) of nonionic surfactant in water, based on the similarity in the critical behavior. This view is also important to elucidate the exact structure of chlorosome, the light-harvesting apparatus of green photosynthetic bacteria, which has currently been of much interest. Since the degree of hydration to nonionic surfactant molecules determines the structure and the phase behavior of the micelle, the Chl aggregation may be controlled by the affinity of the mixed solvent to the molecular structure of Chl or the unit structure of the aggregate colloid. The observed irreversibility in the spectral conversion may arise from particular interaction between Chl and the solvent. The stereochemistry at C13[2] may determine the aggregation behavior by degree of solvation as well as by steric hindrance. Further study on the structure of the Chl *a*′ aggregate colloid is now under way.

Acknowledgment. We are grateful to Dr. M. Konno, Tohoku University (Japan), for TEM and DLS measurements, to Mr. K. Hada, Tokyo, University of Agriculture and Technology (Japan), for help in the experiments, and to Dr. H. Tamiaki, Ritsumeikan University (Japan), for helpful advice.

References and Notes

(1) Deisenhofer, J.; Epp, O.; Miki, K.; Huber, R.; Michel, H. *J. Mol. Biol.* **1984**, *180*, 385−398.
(2) Allen, J. P.; Feher, G.; Yeates, T. O.; Komiya, H.; Rees, D. C. *Proc. Natl. Acad. Sci. U.S.A.* **1987**, *84*, 5730−5734.
(3) Fromme, P.; Witt, H. T.; Schubert, W.-D.; Klulas, O.; Saenger, W.; Krauss, N. *Biochim. Biophys. Acta* **1996**, *1275*, 76−83.
(4) McDermott, G.; Prince, S. M.; Freer, A. A.; Hawthornthwaite-Lawless, A. M.; Papiz, M. Z.; Cogdell, R. J.; Isaacs, N. W. *Nature* **1995**, *374*, 517−521.
(5) Fenna, R. E.; Matthews, B. W. *Nature* **1975**, *258*, 573−577.
(6) Kühlbrandt, W.; Wang, D. N.; Fujiyoshi, Y. *Nature* **1994**, *367*, 614−621.
(7) Katz, J. J.; Bowman, M. K.; Michalski, T. J.; Worcester, D. L. In *Chlorophylls*; Scheer, H., Ed.; CRC Press: Boca Raton, FL, 1991; Chapter 1.8, pp 211−236.
(8) Seely, G. R. In *Primary Processes of Photosynthesis*; Baber, J., Ed.; Elsevier: Amsterdam, 1977; Chapter 1, pp 1−54.
(9) Love, B. B.; Bannister, T. T. *Biophys. J.* **1963**, *3*, 99−113.
(10) Agostiano, A.; Caselli, M.; Della Monica, M.; Gotch, A. J.; Fong, F. K. *Biochim. Biophys. Acta* **1988**, *936*, 171−178.
(11) Jacobs, E. E.; Holt, A. S.; Kromhout, R.; Rabinowitch, E. *Arch. Biochem. Biophys.* **1957**, *72*, 495−511.
(12) Kadoshinikova, I. G.; Kiselev, B. A. *Biofizika* **1979**, *24*, 811−814.
(13) Belavtseva, E. M.; Vorob'yeva, L. M.; Krasnovskii, A. S. *Biofizika* **1959**, *4*, 521−532.
(14) Dijkmans, H. *Eur. J. Chem.* **1973**, *32*, 233−236.
(15) Iriyama, K.; Yoshiura, M. *Colloid Polym. Sci.* **1977**, *255*, 133−139.
(16) Kurawaki, J.; Kusumoto, Y. *Nippon Kagaku Kaishi* **1990**, *1020−1028*.
(17) Gurinovich, G. P.; Strelkova, T. I. *Biofizika* **1968**, *13*, 782−792.
(18) Uehara, K.; Mimuro, M.; Tanaka, M. *Photochem. Photobiol.* **1991**, *53*, 371−377.
(19) Uehara, K.; Hioki, Y.; Mimuro, M. *Photochem. Photobiol.* **1993**, *58*, 127−132.

(20) Oba, T.; Watanabe, T.; Mimuro, M.; Kobayashi, M.; Yoshida, S. *Photochem. Photobiol*. **1996**, *63*, 639−648.

(21) Watanabe, T.; Kobayashi, M.; Hongu, A.; Oba, T. *Chem. Lett*. **1992**, 1847−1850.

(22) Katz, J. J.; Shipman, L. L.; Cotton, T. M.; Janson, T. J. In *Porphyrins*; Dolphin, D., Ed.; Academic Press: New York, 1978; Vol. 5, pp 401−458.

(23) Oksanen, J. A. I.; Helenius, V. M.; Hynninen, P. H.; Van Amerogen, H.; Korppi-Tommola, J. E. I.; Van Grondelle, R. *Photochem. Photobiol*. **1996**, *64*, 356−362.

(24) Scherz, A.; Rosenbach-belkin, V.; Fisher, J. R. E. In *Chlorophylls*; Scheer, H., Ed.; CRC Press: Boca Raton, FL, 1991; Chapter 1.9, pp 237−268.

(25) Maeda, H.; Watanabe, T.; Kobayashi, M.; Ikegami, I. *Biochim. Biophys. Acta* **1992**, *1099*, 74−80.

(26) Oba, T.; Kobayashi, M.; Yoshida, S.; Watanabe, T. *Anal. Sci*. **1996**, *12*, 281−284.

(27) Watanabe, T.; Hongu, A.; Honda, K.; Nakazato, M.; Konno, M.; Saitoh, S. *Anal. Chem.* **1984**, *56*, 251−256.

(28) Weber, G.; Teale, F. W. *Trans. Faraday Soc*. **1959**, *53*, 646−655.

(29) Fujiwara, M.; Tasumi, M. *J. Phys. Chem*. **1986**, *90*, 250−253.

(30) Koyama, Y.; Umemoto, Y.; Akamatsu, A.; Uehara, K.; Tanaka, M. *J. Mol. Struct.* **1986**, *146*, 273−287.

(31) Schaber, P. M.; Hunt, J. E.; Fries, R.; Katz, J. J. *J. Chromatogr*. **1984**, *316*, 25−41.

(32) Shipman, L. L.; Katz, J. J. *J. Phys. Chem*. **1977**, *81*, 577−581.

(33) Nozawa, T.; Ohtomo, K.; Suzuki, M.; Morishita, Y.; Madigan, M. T. *Bull. Chem. Soc. Jpn*. **1993**, *66*, 231−237.

(34) Uehara, K.; Mimuro, M.; Fujita, Y.; Tanaka, M. *Photochem. Photobiol*. **1988**, *48*, 725−732.

(35) Shinoda, K. *J. Colloid Interface Sci.* **1970**, *34*, 278−281.

(36) Lindman, B.; Wennerström, H. *J. Phys. Chem*. **1991**, *95*, 6053−6054.

(37) Chow, H.; Serlin, R.; Strouse, C. E. *J. Am. Chem. Soc*. **1975**, *97*, 7230−7237.